Targeting transcription factor Ascl1 to promote optic nerve regeneration

Bryan Dong[1], Cheng Qi[1], Ximei Luo[2], Jiang Qian[2], Cheng Qian[1, *], Feng-Quan Zhou[1, 3, 4, *]

[1] Department of Orthopedic Surgery, Johns Hopkins University School of Medicine, Baltimore, MD 21205, USA

[2] Department of Ophthalmology, Johns Hopkins University School of Medicine, Baltimore 21205, USA

[3] The Solomon H Snyder Department of Neuroscience, Johns Hopkins University School of Medicine, Baltimore, MD 21205, USA

[4] Sir Run Run Shaw Hospital, Zhejiang University School of Medicine, Hangzhou, China

[*]Corresponding author:

Feng-Quan Zhou, Ph.D., Email: fzhou4@zju.edu.cn

Cheng Qian, Ph.D., Email: cqian5@jhmi.edu

Address: Shang Cheng Qv Qing Chun Dong Lu #3, Hangzhou, China 310016

Abstract

In the adult mammalian CNS neurons, axon regeneration after injury remains limited due to unfavorable intracellular conditions. Factors mediating large-scale epigenetic and transcriptional shifts may be key to driving CNS axon regeneration. Based on previous molecular and gain-of-function studies, we hypothesize that overexpression of *Ascl1* will sufficiently induce robust axon regeneration in adult mammalian CNS neurons.

Introduction:

Axon regeneration of mature neurons in the mammalian central nervous system (CNS) remains virtually absent, presenting a significant biomedical challenge in remediating CNS neural injuries and various neurodegenerative disorders (Qian and Zhou, 2020; Yang et al., 2020). CNS axon regeneration is limited by an inhibitive extrinsic environment and the lack of intrinsic capacities in axon regrowth. Physical barriers, such as glial scars and failure to remove debris remnants (Cregg et al., 2014; Neumann et al., 2008), as well as inhibitory signals, such as myelin associated inhibitors and axon guidance molecules (Giger et al., 2010; Yiu and He, 2006), all constrict axonal growth past the injury site. However, recent studies have indicated that the removal of scarring tissue in either the spinal cord or cerebral cortex (Anderson et al., 2016; Canty et al., 2013), was not sufficient to promote axon regeneration. The prevailing consensus is that a certain intrinsic cellular program, regulating gene transcription and protein expression, is necessary to coordinate the axon regeneration in the CNS. Pinpointing such machinery would therefore be greatly beneficial in more efficient and effective therapies targeting various neurological injuries and diseases.

Upon synaptic connections and neural pathway formation, the developed CNS circuitry greatly attenuates redundant neurite extension and branching. Therefore, the axon regeneration capacity is gradually declined along development (Yang et al., 2022). For example, embryonic and even early postnatal cortical neurons and retinal ganglion cells (RGCs) still possess great potential in neurite outgrowth (Brewer, 1999; Shewan et al., 1995), whereas the adult neurons do not. Along this rationale, several genes required for neural development have been identified as promoters of axon regeneration. Both the transcription factor Sox11 (in Sry-related HMG box family) and Klf6/7 (in Krüppel-like family) have been detected down-regulated across the embryonic-postnatal-adult stages. Unsurprisingly, overexpression of SOX11 or KLF6/7 in adult neurons

augments post-injury axon regeneration in the optic nerve or the corticospinal tract (Hilton and Bradke, 2017; Moore et al., 2009; Wang et al., 2015). On the other hand, deletion of Klf4/9, which is strikingly upregulated along neural maturation and aging, successfully promoted post-injury axon regeneration (Moore et al., 2009). Similarly, downregulation of PTEN, which inhibits the pro-regenerative mTOR pathway common in developing CNS neurons, promotes regeneration of optic nerve and CST axons after injury (Liu et al., 2010; Park et al., 2008).

Terminal regeneration associated genes (RAGs) (Huebner and Strittmatter, 2009; van Kesteren et al., 2011) mediate processes including, but not limited to, cytoskeletal reorganization, changes in protein and lipids metabolism, and modifications to intracellular trafficking, all of which orchestrate the formation of growth cones and axon re-extension (Blanquie and Bradke, 2018; Huebner and Strittmatter, 2009; Wang et al., 2020). Epigenetic regulations, which modify chromatin and gene loci accessibility by coiling and uncoiling the DNA sequence packaged around histones (Lilja et al., 2013; van Steensel, 2011), likely play an important role in regulating multiple RAGs rather than individual RAGs during axon regeneration (Li et al., 2021; Wang et al., 2018a; Wang, 2023). The global level of chromatin accessibility is regulated by either histone tail modification or DNA methylation (Lilja et al., 2013; van Steensel, 2011). Indeed, inhibition of histone deacetylases (HDACs) promotes expression of RAGs and enhances axon regeneration in the CST and PNS (Cho et al., 2013; Finelli et al., 2013), while upregulation of histone acetyltransferases (HATs) promotes intrinsic PNS axonal regrowth (Gaub et al., 2011; Lee and Workman, 2007). Pioneer transcription factors (pTFs) are a distinct class of transcription factors that have an affinity of binding to closed chromatin based on specifically recognized DNA-binding motifs (e.g., high nucleosome occupancy sites) and can recruit complexes to further remodel the epigenetic landscape (Mayran and Drouin, 2018; Zaret and Carroll, 2011). Importantly, pTFs are implicated in the process of reprogramming terminally differentiated cells into a pluripotent state (Iwafuchi-Doi and Zaret, 2014; Iwafuchi-Doi and Zaret, 2016). The application of pTFs in

reprogramming CNS axon regeneration is emerging to be very promising (Venkatesh et al., 2018; Wahane et al., 2019; Yang et al., 2022), given the ability of pTFs to initiate expression of developmentally silenced genes.

Furthermore, neuronal death remains a critical obstacle to functional recovery following CNS injury. In addition to direct injury to the soma, it is well known that trauma to axons impact neuron survival through retrograde signaling mechanisms (Williams et al., 2020). In the adult mammalian retina, around only 20% of RGCs survive 14 days after optic nerve crush (Wang et al., 2018a). Importantly, known axon RAGs do not necessarily promote neuroprotection, as both SOX11 overexpression (Norsworthy et al., 2017) and KLF4 knockout (Moore et al., 2009) did not augment RGC survival rates after optic nerve crush. Therefore, axon regeneration and neuron survivance are two vital but distinct processes in the overall scheme of post-traumatic neuroregeneration. Studies have shown that the application of classical neurotrophic factors (Kimura et al., 2016), and the key neurodevelopment factor WNT (Patel et al., 2017) and apoptosis regulator PTEN (Park et al., 2008), can promote RGC survival post-crush. Though the role of manipulating epigenetics to leverage RGC protection has been explored (Lagali and Picketts, 2011; Tian et al., 2022), the precise patterns of chromatin and DNA accessibility in RGC survival signaling still remains undetermined.

Achaete-scute homolog 1 (ASCL1) is a dimerizing transcription factor belonging to the diverse group of basic helix-loop-helix (bHLH) transcription factors (TFs). ASCL1 is a homolog to the achaete-scute complex (AS-C) discovered in Drosophila melanogaster and it participates in the Notch signaling pathway to regulate neuronal development in both the CNS and PNS (García-Bellido and de Celis, 2009; Ghysen and Dambly-Chaudière, 1988; Romani et al., 1989). As a pTF, ASCL1 recruits an array of proneural factors critical to nervous system development (Castro et al., 2011) and participates in both non-CG DNA methylation and demethylation (Luo et al., 2018).

In vertebrates, ASCL1 is important in directing neurogenesis and neural progenitor differentiation *in vitro* (Raposo et al., 2015), in the spinal cord (Di Bella et al., 2019), and within the cerebral cortex and basal ganglia (Casarosa et al., 1999; Castro et al., 2011). ASCL1 overexpression is also sufficient to promote redifferentiation of Müller glia to neurons in adult mice (Jorstad et al., 2017; Pollak et al., 2013) as well as the induction of mammalian fibroblasts and embryonic stem cells to neurons (Chanda et al., 2014; Luo et al., 2018), showing its potential as a mature cell reprogramming factor. There is some evidence that ASCL1 can drive adult astrocyte to neuron redifferentiation (Liu et al., 2015; Rao et al., 2021), but this specific instance of reprogramming is still hotly contested (Qian et al., 2021; Wang et al., 2021). Although ASCL1 upregulation has been linked to promote dorsal root ganglia (DRG) axon outgrowth in mice (Lisi et al., 2017), and ASCL1 has shown to be upregulated in mature zebrafish RGCs, whose axons can spontaneously regenerate after optic nerve injury (Dhara et al., 2019), the function of ASCL1 in restoring axon regeneration in the mature CNS remains unknown.

In this study, by reanalyzing public available RNA-seq datasets of mouse retinal cells at different developmental and maturation stages, we demonstrated that the transcription levels of many genes known to enhance axon regeneration gradually decrease during tissue maturation, such as *Sox11*, *Ezh2*, *Lin28*, and *Ascl1*. Additional combined bioinformatics analysis of multiomics sequencing identified many transcription factors as potential axon regeneration promotors because they govern the transcription of well-known RAGs either at their promotor or enhancer regions, among which Ascl1 was highly ranked. Importantly, overexpression of Ascl1 in RGCs significantly enhanced optic nerve regeneration and RGCs survival after the optic nerve injury. Moreover, we also identified Sox11 as a potential downstream mediator of Ascl1 to enhance optic nerve regeneration. Collectively, by combining advanced bioinformatics analysis and optic nerve regeneration model our study revealed a new role of Ascl1 in promoting CNS neuronal survival and axon regeneration.

Methods

Mice

All animal experiments were conducted in accordance with the protocol approved by the Institutional Animal Care and Use Committee of Johns Hopkins University. 6-8 week old female CD-1 mice and male C57BL/6J mice were used in animal experiments. The CD-1 wild type mice were ordered from Charles River and the male C57BL/6J mice were ordered from the Jackson Laboratory. All animal surgeries were performed under anesthesia induced by intraperitoneal injection of avertin (20mg/mL) diluted in sterile saline. Details of the surgeries are described below.

Optic nerve regeneration model

Cavities were made just posterior of the ciliary bodies in the right eyes of mice by inserting a 28-gauge needle at a 45-degree angle into the sclera half the length of the needle bevel. 1.5 μL of adenosine-associated virus 2- (AAV2) packaged transgene was injected through the cavity into the vitreous humors using a Hamilton syringe (Model 75 RN Syringe, 30-gauge needle). Care was taken to prevent lens, scleral, and retinal damage by either needle or syringe insertion. 14 days after viral injection, the right optic nerves were exposed laterally by retracting the retractor bulbi muscle and were crushed with Dumont #5 fine forceps (Fine Science Tools) for 10 s at approximately 1.5 mm behind the optic disc. The crush intensity was controlled by applying just enough pressure to ensure the two tips of the forceps were fully closed. 14 days after the optic nerve crush, 1.5 μL of cholera toxin subunit B (CTB) conjugated with Alexa Fluor 594 (2 mg/ml, Thermo Fisher Scientific) was injected into the right vitreous humors of the same mice (same procedure as viral injection) to allow for anterograde tracing of RGC axons in the optic nerves. 2 days after CTB injection, the mice were sacrificed by transcardial perfusion. The right eyeballs were dissected out with the portion of the optic nerve proximal of the optic chiasm remaining attached. The eyes with optic nerves attached were post-fixed in 4% paraformaldehyde (PFA) overnight at 4°C. The optic nerves were then carefully dissected out in 1x phosphate buffered

saline (PBS) to ensure the end of the optic nerve most proximal to the optic disc included the crush site. Optic nerves were then washed three times with PBS to flush out residual PFA. AAV2-GFP was purchased from SignaGen Laboratories. AAV2-EF1a-Ascl1-Flag was packaged by Viagene. All viruses used had titers of 0.5 × 10^13 constructs/mL.

Optic nerve dehydration and clearing

Fixed optic nerves were incubated in stepwise concentrations of tetrahydrofuran (TFH) (steps: 50%, 70%, 80%, 100%, and 100%, v/v % in distilled water, Sigma-Aldrich) in a twelve-well glass plate to dehydrate the nerves. For the final step, nerves were incubated in benzyl alcohol/benzyl benzoate (BABB, 1:2 in volume, Sigma-Aldrich) for tissue clearing. All incubations were performed on an orbital shaker at room temperature for 20 minutes each step, with six steps in total. The dehydrated and cleared optic nerves were mounted in BABB in specialized silica gel wells. The plate was covered in aluminum foil through the entire dehydration and clearing to reduce photobleaching of the optic nerves.

Imaging of RGC axon regeneration

Mounted whole-mount nerves were imaged with a LSM 800 confocal microscope (Zeiss, 20x air objective) with Zeiss ZEN Blue software. The z coordinates of each nerve were first defined by manually adjusting the imaging plane upwards or downwards until signal was no longer observed, demarcating the upper and lower z coordinates, respectively. Then, the Z stack function was used to acquire the range of the z coordinates of the nerve through slices (2 μm) to produce a stack spanning from the lower to upper z coordinates. The x-y coordinates of each nerve were defined by manually tracing the nerve to create imaging tiles that fully encompassed the x-y plane of the nerve. The tiling function (10% overlap) was applied between adjacent tiles to image the whole nerve, such that tiles of each 2 μm-thick slice were stitched to create a complete slice image of the entire nerve. Complete slices could then be combined along the z-axis using Z-stack function.

Analysis of RGC axon regeneration

Quantification of regenerating axons in the optic nerve was performed as previously described (Wang et al., 2018a). Starting from the lower z coordinate, 10 continuous slices were merged along the z-axis to generate a series of 20 μm-thick sections across the entire z-range of the optic nerve. Starting from the crush site (0 μm), distances at 250 μm intervals were drawn, up to 1750 μm from the crush site. At each distance for each 20 μm-thick sections, the number of CTB-labeled axons was counted. For each nerve, the total number of axons at each distance from the crush site was obtained by summing together the number of axons of all 20 μm-thick sections. The maximum diameter of the nerve at each distance was taken to calculate number of axons per micrometer of nerve width, then averaged over all sections. Sad, the total number of axons at distance d in a nerve with a maximum radius of r, was estimated by summing over all optical sections with a thickness of t (20 μm): Sad = πr^2 x (average axons/mm)/t.

Immunohistochemistry of whole-mount retinas

After overnight post-fixation in 4% PFA at 4°C, eyeballs were dissected from the attached optic nerves. Retinas were then carefully dissected from the eyeballs 1x PBS and washed three times in 1x PBS to flush out residual PFA. Retinas were then cut into petal shape (4 opposing radial incisions) and blocked in blocking buffer (1% Triton X-100, 10% goat serum in 1x PBS) for 1 hr at room temperature. Retinas were then stained with primary antibodies (1:500 mouse anti-Tubulin β3, BioLegend) at 4°C, followed by the corresponding Alexa Fluor-conjugated secondary antibodies (1:500, Thermo Fisher Scientific) for 1 hr at room temperature. All antibodies were diluted in blocking buffer. Following both primary and secondary antibody incubation, the retinas were washed in washing buffer (Triton X-100 0.3% in 1x PBS) for four times, for 15 min each time. After the last wash, the retinas were mounted onto slides with ProLong Gold Antifade Mountant with DAPI (Invitrogen).

Analysis of RGC Survival Rate

Eight image fields were selected randomly and imaged from the peripheral regions of each whole-mount retina with a LSM 800 confocal microscope (Zeiss, 20x air objective). RGC survival rate was calculated by dividing the average number of Tuj1+ cells from all eight fields in the injured retinas by that in the uninjured retina. Injured retinas (control and *Ascl1* O/E) were performed under the same timeframe as with the optic nerve regeneration model (16 days after optic nerve crush).

Analysis of RGC Transduction Rate

Uninjured retinas were dissected 14 days after AAV2-GFP injection and fixed in whole-mount, as described above. Six image fields were selected randomly and imaged from the peripheral regions of each whole-mount retina with a LSM 800 confocal microscope (Zeiss, 20x air objective). RGC transduction rate for each image was calculated by counting the number of Tuj1 positive + GFP positive cells and dividing by the number of Tuj1 positive cells.

Immunohistochemistry of retinal cryosections

Retinas were dissected and washed in PBS as described above. Washed retinas were cryoprotected in stepwise sucrose incubations (steps: 10%, 20%, 30%, w/v % in 1x PBS). All steps were performed on the orbital shaker at room temperature until the retinas sunk. Cryoprotected retinas were transferred to plastic molds filled with Tissue-Tek O.C.T. Compound (Sakura), flash frozen on dry ice, and stored at -80°C until cryosectioning. Retinas were then cryosectioned laterally at 10 µm section thickness onto Fisherbrand Superfrost Plus microscope slides (Thermo Fisher) and stored at -20°C until immunostaining. Prior to blocking, slides were warmed at 37°C for 1 hr on a slide blocker. Rectangular barriers around all the sections on a slide were created using a hydrophobic PAP pen (Newcomer Supply) during warming. Slides were

then blocked in blocking buffer (0.3% Triton X-100, 10% goat serum in 1x PBS) for 1 hr, stained with primary antibodies overnight (1:500 mouse anti-Tubulin β3, BioLegend; 1:500 rabbit anti-Sox11, abcam; 1:500 rabbit anti-Sox9, Sigma-Aldrich; 1:250 rabbit anti-Stat3, CST; 1:500 rabbit anti-KLF4, Millipore; 1:250 rabbit anti-pGSK-3β (Ser9), CST; 1:500 rat anti-FLAG, Novus) at 4°C, followed by the corresponding Alexa Fluor-conjugated secondary antibodies (1:500, Thermo Fisher Scientific) for 1 hr at room temperature. All antibodies were diluted in blocking buffer. Following both primary and secondary antibody incubation, the retinas were washed in washing buffer (Triton X-100, 0.3% in 1x PBS) for four times, for 15 min each time. After the last wash, the slides were sealed with ProLong Gold Antifade Mountant with DAPI (Invitrogen).

Analysis of retinal cryosections

Fluorescent images of the retina cryosections were acquired with an Axiovert 200M inverted fluorescent microscope (Zeiss, 20x air objective). For the Ascl1 O/E condition, regions of interest (ROIs) in ImageJ were drawn around Tuj1+ and FLAG+ cells that were counterstained with DAPI. For the control condition, ROIs were drawn around Tuj1+ cells that were counterstained with DAPI. Fluorescent intensity for an image was measured as the mean pixel intensity in ROIs, weighted for the area of ROIs. Average fluorescent intensity was calculated as from 6 images per retina. Normalized intensity was calculated as follows $I_{norm} = (I_{average} - I_{background})/I_{max}$.

Quantification and Statistical Analysis

Statistical analyses were completed with GraphPad Prism 9 and the significance level was set as $p < 0.05$. Data are represented as mean ± standard deviation (error bars) unless specifically stated. For comparisons between two groups, two-tailed unpaired t tests were used. All details regarding statistical analyses, including the tests used, *p*-values, exact values of n, definitions of n, are described in figure legends.

264 **Table 1. Key Resources**

Reagent/resource	Source	Identifier
Antibodies		
Mouse Purified anti-Tubulin β3 (TUBB3) Antibody	BioLegend	Cat# 801202; RRID: AB_ 10063408
Rabbit DYKDDDDK Tag (D6W5B) mAb	Cell Signaling Technology	Cat# 14793; RRID: AB_ 2572291
Rabbit β-Catenin Antibody	Cell Signaling Technology	Cat# 9562; RRID: AB_331149
Rabbit Phospho-Akt (Ser473) (193H12) mAb	Cell Signaling Technology	Cat# 4058S; RRID: AB_ 331168
Rabbit Phospho-GSK-3β (Ser9) Antibody	Cell Signaling Technology	Cat# 9336S; RRID: AB_ 331405
Rabbit Anti-Krueppel-Like Factor 4 (Klf4) Antibody	Sigma-Aldrich	Cat# ABS1514; RRID: AB_ 2313773
Rabbit Stat3 Antibody	Cell Signaling Technology	Cat# 9132; RRID: AB_ 331588
Rabbit PTEN Antibody	Cell Signaling Technology	Cat# 9552S; RRID: AB_ 10694066
Rat anti DYKDDDDK Tag Antibody, clone 6F7	Cell Signaling Technology	Cat# MCA4764; RRID: AB_10598098
Rabbit anti-Sox9 Antibody	Sigma-Aldrich	Cat# AB5535; RRID: AB_2239761
Rabbit recombinant anti-SOX11 antibody	abcam	Cat# ab229185; RRID: AB_2936957
Rabbit Phospho-S6 Ribosomal Protein (Ser235/236) (D57.2.2E) XP® mAb	Cell Signaling Technology	Cat# 4858; RRID: AB_ 916156
Rat DYKDDDDK Epitope Tag Antibody (L5)	Novus Biologicals	Cat# NBP1-06712; RRID: AB_ 1625981
Goat anti-Rabbit IgG (H+L) Cross-Adsorbed Secondary Antibody, Alexa Fluor 488	Thermo Fisher Scientific	Cat# A-11008; RRID: AB_ 143165
Goat anti-Rat IgG (H+L) Cross-Adsorbed Secondary Antibody, Alexa Fluor 568	Thermo Fisher Scientific	Cat# A-11077; RRID: AB_2534121

Reagent/resource	Source	Identifier
Goat anti-Mouse IgG (H+L) Cross-Adsorbed Secondary Antibody, Alexa Fluor 647	Thermo Fisher Scientific	Cat# A-21235; RRID: AB_2535804
Goat anti-Rabbit IgG (H+L) Cross-Adsorbed Secondary Antibody, Alexa Fluor 594	Thermo Fisher Scientific	Cat# A-11012; RRID: AB_ 2534079

Chemicals, Peptides, and Miscellaneous

ProLong Gold Antifade Mountant with DNA Stain DAPI	Thermo Fisher Scientific	Cat# P36931
Alexa Fluor 594-conjugated cholera toxin subunit B	Thermo Fisher Scientific	Cat# C-22842
Goat serum	Sigma-Aldrich	Cat# G9023
Tetrahydrofuran	Sigma-Aldrich	Cat# 186562
Triton X-100	Sigma-Aldrich	Cat# T9284
Benzyl alcohol	Sigma-Aldrich	Cat# 305197
Benzyl benzoate	Sigma-Aldrich	Cat# B6630
Liquid Blocker Super Pap Pen	Newcomer Supply	Cat# 6505
5 µL, Model 75 RN Syringe	Hamilton	Cat# 7634-01
Inox Biology Dumont #5 Forceps	Fine Science Tools	Cat# 11252-20

Recombinant DNA

AAV2-EF1a-Ascl1-Flag	Viagene	N/A
AAV2-GFP	SignaGen Laboratories	N/A

Results

Multi-omics sequencing analysis predicting Ascl1 as a potential factor promoting axon regeneration

Since it has been well known that developmental extension of retinal ganglion cells (RGCs) axons, which bundle into the optic nerve, reaches peak rate (Shigeoka et al., 2016) at early postnatal stages (P0-P5) (diagram in Figure 1A), we first re-analyzed a public dataset (GEO: GSE87064) of an RNA-seq data of whole mouse retinal tissues collected at different developmental stages, from embryonic day 14.5 (E14.5), across postnatal days (P0-P21) (Figure 1B). We validated this RNA-seq data using gene ontology analysis (GO analysis) to summarize whether these differential genes (heatmap in Figure 1B and dot plot in Figure 1C) were either upregulated or downregulated across development. Consistent with our expectation, the genes upregulated across mouse retinal development correspond to, in GO annotations, mature neuronal functions such as visual perception, synaptic functions and membrane potential maintenance (Figure 1I, left); however, the genes downregulated across mouse retinal development, in GO annotations, largely serve more stem cell-like functions (Figure 1I, right).

Specifically, the gene *Ascl1*'s mRNA transcriptional trend was largely unidirectionally declining from embryonic and early postnatal to late postnatal stages (Figure 1D), implying that *Ascl1* might support developmental axon projection. Notably, previously validated axon regeneration promoting factors show similar expression trends as *Ascl1* across mouse retinal development, including *Klf6/7* (Blackmore et al., 2012; Wang et al., 2018b), *Sox11* (Norsworthy et al., 2017), *Jun* (Zhou et al., 2004), *Id2* (Ko et al., 2016), *Myc* (Belin et al., 2015), *Uhrf1* (Oh et al., 2018), etc. (Figure 1E-1H). On the other hand, the factors that have been previously validated to be inhibit axon regeneration, such as *Klf4/9* (Apara et al., 2017; Moore et al., 2009), *Pten* (Weng et al.,

2017) and *Hdac5* (Cho et al., 2013), were shown to be increased in expression in the RNA-seq across mouse retinal development (Figure 1E, 1G-H). Though *Ascl1* expression changes in the same trend with other factors promoting axon regeneration, one cannot conclusively predict that *Ascl1* would enhance CNS post-injury axon regeneration. We then applied the analysis of a public dataset of retinal developmental Assay for Transposase-Accessible Chromatin (ATAC-seq) to more confidently predict that *Ascl1* potentially binds to some gene loci or enhancer regions which are related to known regeneration-associated genes (RAGs). The ATAC-seq analysis, transcription factor (TF)-promoter region prediction and TF-enhancer region prediction were performed in collaboration by Dr. Jiang Qian's lab at the Wilmer Eye Institute at the Johns Hopkins SOM, using their unpublished pipeline and algorithms (Figure 2). We have created a gene list (not shown) representing the high axon regenerative state in the transcriptome that is integrated from a merged pair comparison among some microarray and RNA-seq data, which include upregulated genes after *Klf7*- overexpression (O/E), downregulated genes after *Klf9*- or *Klf6*-O/E in purified mouse RGCs; upregulated genes after *Klf6*-O/E in cortical neurons; upregulated genes after *Sox11*-O/E in purified RGCs and upregulated genes after peripheral nerve injury in adult mouse DRGs (Norsworthy et al., 2017). TFs that regulate, through promoter or enhancer interactions, a higher percentage of genes in this high regenerative transcriptome are ranked with higher priority for further functional validation (Table 1). Among some of these known TFs, which promote CNS axon regeneration, such as *Sox11*, *Myc*, *Fos* and *Id2* (Table 1), the pioneer transcription factor *Ascl1* has been predicted to regulate RAGs at epigenetic level.

Adult mouse optic nerve crush injury model was selected to investigate the effect of Ascl1

We hypothesized that overexpression of *Ascl1* in adult injured CNS neurons could promote axon regeneration. Available CNS-based neuronal culture is commonly using embryonic (E15 or E18) cortical neurons or hippocampal neurons, which all show robust axon outgrowth, since they are

within the embryonic developmental stage. Culturing adult CNS neurons is unfeasible currently, due to inability of cultured CNS neurons to survive. The only adult neurons that can be cultured are dorsal root ganglion neurons, belonging to the PNS, which inherently regenerate robustly after injury. Thus, the mouse optic nerve, a CNS injury model, is the most optimal choice, as it exhibits very limited axon regrowth after injury. This limited spontaneous regenerative character of the optic nerve injury animal model can ideally show axon regeneration after overexpression of Ascl1.

Intravitreal viral injection of AAV2-GFP virus was optimized for transduction efficiency. Tissue dehydration and clearing was performed in order to transparentize the ~200-μm thick mouse optic nerve for confocal microscopy scanning of axons in deep locations within the nerve.

Ascl1 overexpression in RGCs promotes axon regeneration in the adult mouse optic nerve and adult RGC survival after injury

To elucidate the effects of *Ascl1* O/E on adult CNS axon regeneration post-injury, mouse retinas were transduced with AAV2-Ascl1-Flag individually by intravitreal injection. Injection of AAV2-GFP was used as the control group. Optic nerves across all groups were allowed 16 days to regenerate. The results showed that compared to the control group, *Ascl1* O/E significantly enhanced axon regeneration in the optic nerve after crush injury (Figure 3A-B), indicating Ascl1 expression can reprogram adult RGCs into a regeneration-conducive state. Importantly, *Ascl1* O/E allowed for regrowth of axons significantly distal of the crush site (Figure 3A bottom), a phenomenon not observed in the intrinsic regenerative capacity of RGC axons. Thus, overexpression of *Ascl1* in RGCs induces robust axon regeneration in mouse optic nerves post-injury, likely through *Ascl1*-mediated downstream regulation of RAGs. Additionally, we showed that *Ascl1* O/E increases RGC survival rate significantly 16 days after optic nerve injury (Figure 3C-D), implying the role of *Ascl1* as a neuroprotective factor.

***Ascl1* overexpression in RGCs selectively upregulates a known axon regenerative factor but not others**

In order to explicate the mechanisms of *Ascl1*-mediated RGC axon regeneration, mouse retinas were transduced with AAV2-Ascl1-Flag. Injection of 1x PBS was used as the control group. Retinas were harvested 14 days after injection and retinal cryosections were prepared. Retinal cryosections were immunostained against well-known mediators of CNS axon regeneration (Sox11, Sox9, Stat3, KLF4, and pGSK-3β) to see if expression of any targets were mediated *Ascl1* O/E. We found that Sox11 fluorescent intensity in the RGC layer was significantly upregulated in *Ascl1* O/E retinas compared to control (Figure 4A), while fluorescent intensities of other targets were not significantly different between *Ascl1* O/E and control (Figure 4B-E). These results indicate that Sox11 may be downstream of Ascl1 signaling and influence its pro-regenerative effects.

Figure legends

Figure 1. RGC axon growth in correspondence with differential gene expression across mouse retinal development.

(A) Diagram showing the expression of axon guidance-related molecules and functional stages of RGC axon growth are closely related to the mouse embryonic and postnatal developmental stages. (B) Heatmap revealing the whole-genome gene differential pattern across mouse retinal development (raw RNA-seq data is from public dataset GSE87064). (C) Dot plot indicating variable gene expression and cell coverage of various axon regeneration promoting factors across purified RGC development (raw scRNA-seq data is from public dataset GSE185671). (D)-(H) Line graphs showing the trend of *Ascl1* expression across retinal development is consistent with several known promoting factors to axon regeneration; meanwhile, the trend of *Ascl1* expression across retinal development is opposite to known inhibitive factors to axon regeneration. The relative mRNA transcription level was normalized to the highest stage. (I) Gene ontology summarizing the functions of genes upregulated (left) or downregulated (right) across mouse retinal development.

Figure 2. Mouse retinal development corresponds to differential chromatin states.

(A) Heatmap (ATAC-seq) showing the transition of developmentally open or closed genomic regions (peaks) in mouse retina across embryonic and postnatal stages. The number on the left of each differential pattern indicates the quantification of peaks. (B) Pie chart revealing the genomic nature of all differential peaks shown in (A). (C) Diagram illustrating the method using H3K27Ac and H3K4me1 ChIP-seq for characterizing active enhancer regions among all peaks shown in (A). (D) Heatmap showing differential patterns of all enhancer peaks extracted from (A). The number on the left of each differential pattern indicates the quantification of enhancer peaks. All ATAC-seq and ChIP-seq raw data were obtained from the public dataset GSE87064.

Figure 3. *Ascl1* overexpression in adult RGCs drives axon regeneration and increases survival rate after optic nerve injury.

(A) Top: timeline of the experiment. Middle: representative images showing that *Ascl1* O/E in adult RGCs promotes substantial axon regeneration in optic nerves 16 days after optic nerve crush compared to the control group. The red line indicates the crush sites. The red arrows indicate the longest axons of each nerve. White scale bars are 100 μm in length. Bottom: Enlarged images of sections of nerves at 100 μm, 250 μm, 500 μm, and 750 μm distal of the crush sites. (B) Bar chart showing quantification of (A). A dot represents an individual optic nerve [n = 7 mice in the 16 day injection-to-crush control group, n = 8 mice in the 16 day injection-to-crush *Ascl1* O/E group]. Unpaired *t*-tests were applied at all distances [$p < 0.0001$ at 250 μm, 500 μm, and 750 μm; $p = 0.0005$ at 1000 μm; $p = 0.002$ at 1250 μm; $p = 0.0104$ at 1500 μm; $p = 0.0727$ at 1750 μm]. (C) Representative image fields of whole mount retinas showing that *Ascl1* O/E in adult RGCs significantly increased RGC survival rate 16 days after optic nerve crush compared to the control group. From left, sham no injury retina, control group retina 16 days after optic nerve crush, *Ascl1* O/E retina 16 days after optic nerve crush. Whole-mount retinas were stained with anti-βIII tubulin (Tuj1, green channel) antibodies. White scale bars are 50 μm in length. (D) Scatter plot showing quantification of (C). An unpaired *t*-test was applied [$p = 0.0001$]. n = 6 mice in the 16 day injection-to-crush control group, n = 6 mice in the 16 day injection-to-crush *Ascl1* O/E group). ns not significant. * $p < 0.05$, ** $p < 0.01$, *** $p < 0.001$, **** $p < 0.0001$.

Figure 4. ASCL1 overexpression upregulates SOX11 but does not mediate other regenerative factors in adult RGCs after optic nerve crush

A) Representative images indicating greater SOX11 intensity in the RGC layer under Ascl1 O/E two days after ONC. Retinal cryosections were stained with DAPI (blue), anti-SOX11 (green), anti-FLAG (red) and anti-tubulin β3 (far-red) antibodies. The white scale bar is 50 μm.

Bottom right is quantification of normalized intensity (unpaired T-test, $p = 0.0007$, n = 5 retinas for control, n = 4 retinas for Ascl1 O/E). B) Representative images indicating no significant difference in SOX9 intensity between Tuj1+ and FLAG+ Ascl1 O/E cells and Tuj1+ control cells (unpaired T-test, $p = 0.0825$, n = 6 retinas for control, n = 4 retinas for Ascl1 O/E). C) Representative images indicating no significant difference in STAT3 intensity between Tuj1+ and FLAG+ Ascl1 O/E cells and Tuj1+ control cells (unpaired T-test, $p = 0.0990$, n = 6 retinas for control, n = 4 retinas for Ascl1 O/E). D) Representative images indicating no significant difference in KLF4 intensity between Tuj1+ and FLAG+ Ascl1 O/E cells and Tuj1+ control cells (unpaired T-test, $p = 0.3766$, n = 6 retinas for control, n = 4 retinas for Ascl1 O/E). E) Representative images indicating no significant difference in pGSK3β intensity between Tuj1+ and FLAG+ Ascl1 O/E cells and Tuj1+ control cells (unpaired T-test, $p = 0.7996$, n = 6 retinas for control, n = 4 retinas for Ascl1 O/E) ns not significant. *** $p < 0.001$. Representative images from the Ascl1 O/E were normalized such that $I_{background}$ was equal to that of the control condition.

Figure 5 (Supplementary). AAV2-GFP transduction rate in RGCs

(A) Representative image field of a whole mount retina showing AAV2 GFP transduction rate in RGCs. From left, GFP single channel, Tuj1 single channel, combined Tuj1 (red) + GFP (green) channels. Whole-mount retinas were stained with anti-βIII tubulin (Tuj1, red channel) antibodies. White scale bars are 50 μm in length. (B) Quantification of the transduction rate of AAV2 GFP in RGCs in (A). The average transduction rate was 81.416 ± 2.496%. The bars on the graph represent standard deviation. A dot represents an individual retina [n = 4 mice].

Table 2. Candidate list of predicted developmentally differential TFs regulating RAGs.

Rank	TFs regulate RAGs via promoters	TFs regulate RAGs via enhancers
1	*Confidential**	*Confidential*
2	*Confidential **	*Confidential **
3	*Confidential*	*Confidential **
4	*Confidential*	*Confidential*
5	Fos	*Confidential*
6	*Confidential*	Fos
7	*Confidential*	*Confidential*
8	Sox2*	*Confidential*
9	Sox11*	*Confidential*
10	*Confidential*	Myc
11	*Confidential*	*Confidential*
12	*Confidential **	*Confidential **
13	*Confidential **	*Confidential **
14	*Confidential*	*Confidential*
15	*Confidential **	*Confidential*
16	*Confidential*	*Confidential*
17	*Confidential*	*Confidential*
18	*Confidential*	*Confidential*
19	*Confidential*	*Confidential*
20	*Confidential*	*Confidential*
21	*Confidential*	**Ascl1***
22	*Confidential*	Id2
23	**Ascl1***	*Confidential **

24	*Confidential*	*Confidential*
25	*Confidential*	*Confidential*
26	*Confidential*	*Confidential*
27	*Confidential*	*Confidential*
28	*Confidential*	*Confidential*
29	*Confidential*	*Confidential*
30	Id2	*Confidential*

* TF with pioneer activity.

Discussion

After development into maturity, CNS neurons transition from an inducible growth state to a permanently regeneration-inhibitory condition (Shewan et al., 1995). A growing consensus indicates that, similarly to the processes of cell differentiation and the reprogramming of somatic cells to induced pluripotent stem cells (iPSCs), epigenetic modifications can be utilized to the CNS genome in response to injury in order to promote axon regeneration (Gaub et al., 2010; Lindner et al., 2013; Wahane et al., 2019). Indeed, the RGC axon regeneration data indicate that ASCL1 is an important factor in inducing CNS axon regeneration within RGCs and the optic nerve and support the idea that adult CNS neurons can be feasibly reprogrammed into a pro-regenerative state. Previous studies have shown that ASCL1 overexpression has been implicated in reprogramming adult GABAergic cortical neurons to dopaminergic cortical neurons (Raina et al., 2019) and in differentiating human pluripotent stem cells into GABAergic neurons (Yang et al., 2017), demonstrating the capability of ASCL1 to extensively remodel the genomic landscape in neuronal reprogramming. ASCL1 operates in cohort with other factors, such as DNA binding protein Id4 (Blomfield et al., 2019), nuclear receptor transcriptional factor NURR1 (Raina et al., 2019), and microRNA miR-124-9-9 (Wohl and Reh, 2016), to access and open certain regions on the chromatin landscape. Thus, it is likely that ASCL1 overexpression in the CNS facilitates chromatin accessibility, leading to the expression of RAGs which promote axon regeneration.

The retinal cryosection immunostaining data implicate SOX11 as one of the RAGs downstream of ASCL1. SOX11 is a member of the SRY-related high mobility group box transcription factor family and has been implicated as a master regulator of key steps in neurodevelopment, such as proliferation, neurogenesis, and migration (Bergsland et al., 2006; Wang et al., 2013). Importantly, endogenous SOX11 signaling is necessary for the intrinsic adult PNS axon regenerative response following injury (Jankowski et al., 2009), while SOX11 overexpression has been shown to promote

axon regeneration in mature saphenous nerve (Jing et al., 2012), optic nerve (Norsworthy et al., 2017), and corticospinal tract mouse models (Wang et al., 2015). Interestingly, SOX11 signaling is downstream of ASCL1 and related bHLH class TFs Ngn2 and NeuroM/Math3 during neurodevelopment (Bergsland et al., 2006). Furthermore, ASCL1-mediated astrocyte-to-neuron conversion was accompanied with an increase in SOX11 expression (Rao et al., 2021). These studies suggest that ASCL1-induced RGC axon regeneration is partially dependent on SOX11 pathways

However, the definite locations on the chromatin which ASCL1 interacts with, and the downstream targets that ASCL1 expression mediates remain unknown. Therefore, it would be beneficial to utilize recent advances in nucleic acid/chromatin sequencing to further elucidate the mechanisms of ASCL1 in promoting a regenerative environment. Specifically, chromatin immunoprecipitation followed by sequencing (ChIP-seq), a technique that maps DNA-protein interactions on the genomic level (Orgeur et al., 2017; Park, 2009), can be used to find the sites which ASCL1 binds to chromatin while Assay for Transposase-Accessible Chromatin using sequencing (ATAC-seq), a technique that locates accessible DNA locations on the entire chromatin landscape (Buenrostro et al., 2013), can be utilized to elucidate the regions that are affected by ASCL1 expression. Thus, the application of ChIP-seq and ATAC-seq in combination can identify the precise downstream targets of ASCL1, which can be manipulated with ASCL1 overexpression to further enhance CNS axon regrowth. Indeed, previous studies have indicated that synergistic reprogramming of neurons by manipulating multiple targets has an additive, combinatory effect on enhancing axon regeneration (Norsworthy et al., 2017; Wang et al., 2018a). Additionally, further -omics analysis, with improvements in RGC subtype distinction, sequencing depth and coverage (Tran et al., 2019), may be useful to greater elucidate the downstream pathways associated with ASCL1 in the CNS axon regeneration paradigm.

In the paradigm of axon regeneration, it is known that many RAGs are either proto-oncogenes, or participate in signaling pathways found in tumorous cells. Abnormal expression of RAGs such as p300, PTEN, and the Klf family of proteins have been purported in mediating a myriad of different forms of cancer (Liu et al., 2019; Milella et al., 2015; Tetreault et al., 2013). Misfunction of the PI3K/Akt signaling pathway which ASCL1 mediates (Dong et al., 2019) is implicated in a variety of cancers (Janku et al., 2018). Furthermore, elevated levels of ASCL1 remains a potent biomarker in small cell lung cancer (Furuta et al., 2019; Rudin et al., 2019). However, a study has found that ASCL1-induced differentiation inhibited the progression of human glioma cells (Cheng et al., 2019). The exact mechanisms in which ASCL1 mediates tumor development and progression remains unknown, and any attempts of ASCL1 reprogramming should account for these potential consequences. Nonetheless, with regards to epigenetic reprogramming in axon regeneration, pTFs such as ASCL1 are greatly advantageous to alterations using global epigenetic modifications (HATs, HDACs). PTFs importantly bind to specific sequences on chromatin (Zaret and Carroll, 2011), while many HATs and HDACs change the chromatin structure across the entire genome (Katan-Khaykovich and Struhl, 2002), potentially altering the expression of many targets that do not participate in driving axon regeneration, thereby leading to unintended consequences. The precise mechanisms of PTF/chromatin binding should be pursued in cellular reprogramming as the leading standard to alleviate off-target epigenetic expression.

References

Anderson, M.A., J.E. Burda, Y. Ren, Y. Ao, T.M. O'Shea, R. Kawaguchi, G. Coppola, B.S. Khakh, T.J. Deming, and M.V. Sofroniew. 2016. Astrocyte scar formation aids central nervous system axon regeneration. *Nature*. 532:195-200.

Apara, A., J. Galvao, Y. Wang, M. Blackmore, A. Trillo, K. Iwao, D.P. Brown, K.A. Fernandes, A. Huang, T. Nguyen, M. Ashouri, X. Zhang, P.X. Shaw, N.J. Kunzevitzky, D.L. Moore, R.T. Libby, and J.L. Goldberg. 2017. KLF9 and JNK3 Interact to Suppress Axon Regeneration in the Adult CNS. *The Journal of Neuroscience*. 37:9632-9644.

Belin, S., H. Nawabi, C. Wang, S. Tang, A. Latremoliere, P. Warren, H. Schorle, C. Uncu, C.J. Woolf, Z. He, and J.A. Steen. 2015. Injury-Induced Decline of Intrinsic Regenerative Ability Revealed by Quantitative Proteomics. *Neuron*. 86:1000-1014.

Bergsland, M., M. Werme, M. Malewicz, T. Perlmann, and J. Muhr. 2006. The establishment of neuronal properties is controlled by Sox4 and Sox11. *Genes Dev*. 20:3475-3486.

Blackmore, M.G., Z. Wang, J.K. Lerch, D. Motti, Y.P. Zhang, C.B. Shields, J.K. Lee, J.L. Goldberg, V.P. Lemmon, and J.L. Bixby. 2012. Krüppel-like Factor 7 engineered for transcriptional activation promotes axon regeneration in the adult corticospinal tract. *Proceedings of the National Academy of Sciences*. 109:7517-7522.

Blanquie, O., and F. Bradke. 2018. Cytoskeleton dynamics in axon regeneration. *Current Opinion in Neurobiology*. 51:60-69.

Blomfield, I.M., B. Rocamonde, M.D.M. Masdeu, E. Mulugeta, S. Vaga, D.L. van den Berg, E. Huillard, F. Guillemot, and N. Urbán. 2019. Id4 promotes the elimination of the pro-activation factor Ascl1 to maintain quiescence of adult hippocampal stem cells. *Elife*. 8.

Brewer, G.J. 1999. Regeneration and Proliferation of Embryonic and Adult Rat Hippocampal Neurons in Culture. *Experimental Neurology*. 159:237-247.

Buenrostro, J.D., P.G. Giresi, L.C. Zaba, H.Y. Chang, and W.J. Greenleaf. 2013. Transposition of native chromatin for fast and sensitive epigenomic profiling of open chromatin, DNA-binding proteins and nucleosome position. *Nature Methods*. 10:1213-1218.

Canty, A.J., L. Huang, J.S. Jackson, G.E. Little, G. Knott, B. Maco, and V. De Paola. 2013. In-vivo single neuron axotomy triggers axon regeneration to restore synaptic density in specific cortical circuits. *Nature Communications*. 4.

Casarosa, S., C. Fode, and F. Guillemot. 1999. Mash1 regulates neurogenesis in the ventral telencephalon. *Development*. 126:525-534.

Castro, D.S., B. Martynoga, C. Parras, V. Ramesh, E. Pacary, C. Johnston, D. Drechsel, M. Lebel-Potter, L.G. Garcia, C. Hunt, D. Dolle, A. Bithell, L. Ettwiller, N. Buckley, and F. Guillemot. 2011. A novel function of the proneural factor Ascl1 in progenitor proliferation identified by genome-wide characterization of its targets. *Genes & Development*. 25:930-945.

Chanda, S., Cheen E. Ang, J. Davila, C. Pak, M. Mall, Qian Y. Lee, H. Ahlenius, Seung W. Jung, Thomas C. Südhof, and M. Wernig. 2014. Generation of Induced Neuronal Cells by the Single Reprogramming Factor ASCL1. *Stem Cell Reports*. 3:282-296.

Cheng, X., Z. Tan, X. Huang, Y. Yuan, S. Qin, Y. Gu, D. Wang, C. He, and Z. Su. 2019. Inhibition of Glioma Development by ASCL1-Mediated Direct Neuronal Reprogramming. *Cells*. 8:571.

Cho, Y., R. Sloutsky, Kristen M. Naegle, and V. Cavalli. 2013. Injury-Induced HDAC5 Nuclear Export Is Essential for Axon Regeneration. *Cell*. 155:894-908.

Cregg, J.M., M.A. DePaul, A.R. Filous, B.T. Lang, A. Tran, and J. Silver. 2014. Functional regeneration beyond the glial scar. *Experimental Neurology*. 253:197-207.

Dhara, S.P., A. Rau, M.J. Flister, N.M. Recka, M.D. Laiosa, P.L. Auer, and A.J. Udvadia. 2019. Cellular reprogramming for successful CNS axon regeneration is driven by a temporally changing cast of transcription factors. *Scientific Reports*. 9.

Di Bella, D.J., A.L. Carcagno, M.L. Bartolomeu, M.B. Pardi, H. Löhr, N. Siegel, M. Hammerschmidt, A. Marín-Burgin, and G.M. Lanuza. 2019. Ascl1 Balances Neuronal versus Ependymal Fate in the Spinal Cord Central Canal. *Cell Reports*. 28:2264-2274.e2263.

Dong, Z.-y., Z. Pei, Y.-l. Wang, Z. Li, A. Khan, and X.-t. Meng. 2019. Ascl1 Regulates Electric Field-Induced Neuronal Differentiation Through PI3K/Akt Pathway. *Neuroscience*. 404:141-152.

Finelli, M.J., J.K. Wong, and H. Zou. 2013. Epigenetic Regulation of Sensory Axon Regeneration after Spinal Cord Injury. *The Journal of Neuroscience*. 33:19664-19676.

Furuta, M., J. Sakakibara-Konishi, H. Kikuchi, H. Yokouchi, H. Nishihara, H. Minemura, M. Harada, S. Yamazaki, K. Akie, Y. Fujita, K. Takamura, T. Kojima, T. Harada, Y. Minami, N. Watanabe, S. Oizumi, H. Suzuki, M. Nishimura, H. Dosaka-Akita, and H. Isobe. 2019. Analysis of DLL3 and ASCL1 in Surgically Resected Small Cell Lung Cancer (HOT1702). *The Oncologist*. 24:e1172-e1179.

García-Bellido, A., and J.F. de Celis. 2009. The Complex Tale of the achaete–scute Complex: A Paradigmatic Case in the Analysis of Gene Organization and Function During Development. *Genetics*. 182:631-639.

Gaub, P., Y. Joshi, A. Wuttke, U. Naumann, S. Schnichels, P. Heiduschka, and S. Di Giovanni. 2011. The histone acetyltransferase p300 promotes intrinsic axonal regeneration. *Brain*. 134:2134-2148.

Gaub, P., A. Tedeschi, R. Puttagunta, T. Nguyen, A. Schmandke, and S. Di Giovanni. 2010. HDAC inhibition promotes neuronal outgrowth and counteracts growth cone collapse through CBP/p300 and P/CAF-dependent p53 acetylation. *Cell Death & Differentiation*. 17:1392-1408.

Ghysen, A., and C. Dambly-Chaudière. 1988. From DNA to form: the achaete-scute complex. *Genes & Development*. 2:495-501.

Giger, R.J., E.R. Hollis, and M.H. Tuszynski. 2010. Guidance Molecules in Axon Regeneration. *Cold Spring Harbor Perspectives in Biology*. 2:a001867-a001867.

Hilton, B.J., and F. Bradke. 2017. Can injured adult CNS axons regenerate by recapitulating development? *Development*. 144:3417-3429.

Huebner, E.A., and S.M. Strittmatter. 2009. Axon Regeneration in the Peripheral and Central Nervous Systems. *In* Results and Problems in Cell Differentiation. Springer Berlin Heidelberg. 305-360.

Iwafuchi-Doi, M., and K.S. Zaret. 2014. Pioneer transcription factors in cell reprogramming. *Genes & Development*. 28:2679-2692.

Iwafuchi-Doi, M., and K.S. Zaret. 2016. Cell fate control by pioneer transcription factors. *Development*. 143:1833-1837.

Jankowski, M.P., S.L. McIlwrath, X. Jing, P.K. Cornuet, K.M. Salerno, H.R. Koerber, and K.M. Albers. 2009. Sox11 transcription factor modulates peripheral nerve regeneration in adult mice. *Brain Res*. 1256:43-54.

Janku, F., T.A. Yap, and F. Meric-Bernstam. 2018. Targeting the PI3K pathway in cancer: are we making headway? *Nature Reviews Clinical Oncology*. 15:273-291.

Jing, X., T. Wang, S. Huang, J.C. Glorioso, and K.M. Albers. 2012. The transcription factor Sox11 promotes nerve regeneration through activation of the regeneration-associated gene Sprr1a. *Exp Neurol*. 233:221-232.

Jorstad, N.L., M.S. Wilken, W.N. Grimes, S.G. Wohl, L.S. VandenBosch, T. Yoshimatsu, R.O. Wong, F. Rieke, and T.A. Reh. 2017. Stimulation of functional neuronal regeneration from Müller glia in adult mice. *Nature*. 548:103-107.

Katan-Khaykovich, Y., and K. Struhl. 2002. Dynamics of global histone acetylation and deacetylation in vivo: rapid restoration of normal histone acetylation status upon removal of activators and repressors. *Genes & Development*. 16:743-752.

Kimura, A., K. Namekata, X. Guo, C. Harada, and T. Harada. 2016. Neuroprotection, Growth Factors and BDNF-TrkB Signalling in Retinal Degeneration. *International Journal of Molecular Sciences*. 17:1584.

Ko, H.R., I.-S. Kwon, I. Hwang, E.-J. Jin, J.-H. Shin, A.M. Brennan-Minnella, R. Swanson, S.-W. Cho, K.-H. Lee, and J.-Y. Ahn. 2016. Akt1-Inhibitor of DNA binding2 is essential for growth cone formation and axon growth and promotes central nervous system axon regeneration. *eLife*. 5.

Lagali, P.S., and D.J. Picketts. 2011. Matters of life and death: the role of chromatin remodeling proteins in retinal neuron survival. *Journal of Ocular Biology, Diseases, and Informatics*. 4:111-120.

Lee, K.K., and J.L. Workman. 2007. Histone acetyltransferase complexes: one size doesn't fit all. *Nature Reviews Molecular Cell Biology*. 8:284-295.

Li, Q., C. Qian, H. Feng, T. Lin, Q. Zhu, Y. Huang, and F.Q. Zhou. 2021. N6-methyladenine DNA Demethylase ALKBH1 Regulates Mammalian Axon Regeneration. *Neurosci Bull*. 37:809-814.

Lilja, T., N. Heldring, and O. Hermanson. 2013. Like a rolling histone: Epigenetic regulation of neural stem cells and brain development by factors controlling histone acetylation and methylation. *Biochimica et Biophysica Acta (BBA) - General Subjects*. 1830:2354-2360.

Lindner, R., R. Puttagunta, and S. Di Giovanni. 2013. Epigenetic Regulation of Axon Outgrowth and Regeneration in CNS Injury: The First Steps Forward. *Neurotherapeutics*. 10:771-781.

Lisi, V., B. Singh, M. Giroux, E. Guzman, M.W. Painter, Y.-C. Cheng, E. Huebner, G. Coppola, M. Costigan, C.J. Woolf, and K.S. Kosik. 2017. Enhanced neuronal regeneration in the CAST/Ei mouse strain is linked to expression of differentiation markers after injury. Cold Spring Harbor Laboratory.

Liu, K., Y. Lu, J.K. Lee, R. Samara, R. Willenberg, I. Sears-Kraxberger, A. Tedeschi, K.K. Park, D. Jin, B. Cai, B. Xu, L. Connolly, O. Steward, B. Zheng, and Z. He. 2010. PTEN deletion enhances the regenerative ability of adult corticospinal neurons. *Nature Neuroscience*. 13:1075-1081.

Liu, Y., Q. Miao, J. Yuan, S. Han, P. Zhang, S. Li, Z. Rao, W. Zhao, Q. Ye, J. Geng, X. Zhang, and L. Cheng. 2015. Ascl1 Converts Dorsal Midbrain Astrocytes into Functional Neurons In Vivo. *Journal of Neuroscience*. 35:9336-9355.

Liu, Z., Y. He, X. Lian, H. Zou, Y. Huang, N. Wang, J. Hu, X. Cui, J. Zhao, W. Zhang, W. Gu, L. Pang, and Y. Qi. 2019. Prognostic role of upregulated P300 expression in human cancers: A clinical study of synovial sarcoma and a meta-analysis. *Experimental and Therapeutic Medicine*.

Luo, C., Q.Y. Lee, O. Wapinski, R. Castanon, J.R. Nery, M. Mall, M.S. Kareta, S.M. Cullen, M.A. Goodell, H.Y. Chang, M. Wernig, and J.R. Ecker. 2018. Author response: Global DNA methylation remodeling during direct reprogramming of fibroblasts to neurons. eLife Sciences Publications, Ltd.

Mayran, A., and J. Drouin. 2018. Pioneer transcription factors shape the epigenetic landscape. *Journal of Biological Chemistry*. 293:13795-13804.

Milella, M., I. Falcone, F. Conciatori, U. Cesta Incani, A. Del Curatolo, N. Inzerilli, C.M.A. Nuzzo, V. Vaccaro, S. Vari, F. Cognetti, and L. Ciuffreda. 2015. PTEN: Multiple Functions in Human Malignant Tumors. *Frontiers in Oncology*. 5.

Moore, D.L., M.G. Blackmore, Y. Hu, K.H. Kaestner, J.L. Bixby, V.P. Lemmon, and J.L. Goldberg. 2009. KLF Family Members Regulate Intrinsic Axon Regeneration Ability. *Science*. 326:298-301.

Neumann, H., M.R. Kotter, and R.J.M. Franklin. 2008. Debris clearance by microglia: an essential link between degeneration and regeneration. *Brain*. 132:288-295.

Norsworthy, M.W., F. Bei, R. Kawaguchi, Q. Wang, N.M. Tran, Y. Li, B. Brommer, Y. Zhang, C. Wang, J.R. Sanes, G. Coppola, and Z. He. 2017. Sox11 Expression Promotes Regeneration of Some Retinal Ganglion Cell Types but Kills Others. *Neuron*. 94:1112-1120.e1114.

Oh, Y.M., M. Mahar, E.E. Ewan, K.M. Leahy, G. Zhao, and V. Cavalli. 2018. Epigenetic regulator UHRF1 inactivates REST and growth suppressor gene expression via DNA methylation to promote axon regeneration. *Proceedings of the National Academy of Sciences*. 115.

Orgeur, M., M. Martens, G. Leonte, S. Nassari, M.-A. Bonnin, S.T. Börno, B. Timmermann, J. Hecht, D. Duprez, and S. Stricker. 2017. Genome-wide strategies identify molecular niches regulated by connective tissue-associated transcription factors. Cold Spring Harbor Laboratory.

Park, K.K., K. Liu, Y. Hu, P.D. Smith, C. Wang, B. Cai, B. Xu, L. Connolly, I. Kramvis, M. Sahin, and Z. He. 2008. Promoting Axon Regeneration in the Adult CNS by Modulation of the PTEN/mTOR Pathway. *Science*. 322:963-966.

Park, P.J. 2009. ChIP–seq: advantages and challenges of a maturing technology. *Nature Reviews Genetics*. 10:669-680.

Patel, A.K., K.K. Park, and A.S. Hackam. 2017. Wnt signaling promotes axonal regeneration following optic nerve injury in the mouse. *Neuroscience*. 343:372-383.

Pollak, J., M.S. Wilken, Y. Ueki, K.E. Cox, J.M. Sullivan, R.J. Taylor, E.M. Levine, and T.A. Reh. 2013. ASCL1 reprograms mouse Müller glia into neurogenic retinal progenitors. *Development*. 140:2619-2631.

Qian, C., B. Dong, X.Y. Wang, and F.Q. Zhou. 2021. In vivo glial trans-differentiation for neuronal replacement and functional recovery in central nervous system. *The FEBS Journal*. 288:4773-4785.

Qian, C., and F.Q. Zhou. 2020. Updates and challenges of axon regeneration in the mammalian central nervous system. *Journal of Molecular Cell Biology*. in press.

Raina, A., S. Mahajani, M. Bähr, and S. Kügler. 2019. Neuronal Trans-differentiation by Transcription Factors Ascl1 and Nurr1: Induction of a Dopaminergic Neurotransmitter Phenotype in Cortical GABAergic Neurons. *Molecular Neurobiology*. 57:249-260.

Rao, Z., R. Wang, S. Li, Y. Shi, L. Mo, S.e. Han, J. Yuan, N. Jing, and L. Cheng. 2021. Molecular Mechanisms Underlying Ascl1-Mediated Astrocyte-to-Neuron Conversion. *Stem Cell Reports*. 16:534-547.

Raposo, Alexandre A.S.F., Francisca F. Vasconcelos, D. Drechsel, C. Marie, C. Johnston, D. Dolle, A. Bithell, S. Gillotin, Debbie L.C. van den Berg, L. Ettwiller, P. Flicek, Gregory E. Crawford, Carlos M. Parras, B. Berninger, Noel J. Buckley, F. Guillemot, and Diogo S. Castro. 2015. Ascl1 Coordinately Regulates Gene Expression and the Chromatin Landscape during Neurogenesis. *Cell Reports*. 10:1544-1556.

Romani, S., S. Campuzano, E.R. Macagno, and J. Modolell. 1989. Expression of achaete and scute genes in Drosophila imaginal discs and their function in sensory organ development. *Genes & Development*. 3:997-1007.

Rudin, C.M., J.T. Poirier, L.A. Byers, C. Dive, A. Dowlati, J. George, J.V. Heymach, J.E. Johnson, J.M. Lehman, D. MacPherson, P.P. Massion, J.D. Minna, T.G. Oliver, V. Quaranta, J. Sage, R.K. Thomas, C.R. Vakoc, and A.F. Gazdar. 2019. Molecular subtypes of small cell lung cancer: a synthesis of human and mouse model data. *Nature Reviews Cancer*. 19:289-297.

Shewan, D., M. Berry, and J. Cohen. 1995. Extensive regeneration in vitro by early embryonic neurons on immature and adult CNS tissue. *The Journal of Neuroscience*. 15:2057-2062.

Shigeoka, T., H. Jung, J. Jung, B. Turner-Bridger, J. Ohk, Julie Q. Lin, Paul S. Amieux, and Christine E. Holt. 2016. Dynamic Axonal Translation in Developing and Mature Visual Circuits. *Cell*. 166:181-192.

Tetreault, M.-P., Y. Yang, and J.P. Katz. 2013. Krüppel-like factors in cancer. *Nature Reviews Cancer*. 13:701-713.

Tian, F., Y. Cheng, S. Zhou, Q. Wang, A. Monavarfeshani, K. Gao, W. Jiang, R. Kawaguchi, Q. Wang, M. Tang, R. Donahue, H. Meng, A. Jacobi, J. Yin, X. Cai, S. Hegarty, J. Stanicka, P. Dmitriev, D. Taub, C.J. Woolf, J.R. Sanes, D.H. Geschwind, and Z. He. 2022. Core Transcription Programs Controlling Injury-Induced Neurodegeneration of Retinal Ganglion Cells. Cold Spring Harbor Laboratory.

Tran, N.M., K. Shekhar, I.E. Whitney, A. Jacobi, I. Benhar, G. Hong, W. Yan, X. Adiconis, M.E. Arnold, J.M. Lee, J.Z. Levin, D. Lin, C. Wang, C.M. Lieber, A. Regev, Z. He, and J.R. Sanes. 2019. Single-Cell Profiles of Retinal Ganglion Cells Differing in Resilience to Injury Reveal Neuroprotective Genes. *Neuron*. 104:1039-1055.e1012.

van Kesteren, R.E., M.R.J. Mason, H.D. MacGillavry, A.B. Smit, and J. Verhaagen. 2011. A Gene Network Perspective on Axonal Regeneration. *Frontiers in Molecular Neuroscience*. 4.

van Steensel, B. 2011. Chromatin: constructing the big picture. *The EMBO Journal*. 30:1885-1895.

Venkatesh, I., V. Mehra, Z. Wang, B. Califf, and M.G. Blackmore. 2018. Developmental chromatin restriction of pro-growth gene networks acts as an epigenetic barrier to axon regeneration in cortical neurons. Cold Spring Harbor Laboratory.

Wahane, S., D. Halawani, X. Zhou, and H. Zou. 2019. Epigenetic Regulation Of Axon Regeneration and Glial Activation in Injury Responses. *Frontiers in Genetics*. 10.

Wang, L.-L., C. Serrano, X. Zhong, S. Ma, Y. Zou, and C.-L. Zhang. 2021. Revisiting astrocyte to neuron conversion with lineage tracing in vivo. *Cell*. 184:5465-5481.e5416.

Wang, X.-W., Q. Li, C.-M. Liu, P.A. Hall, J.-J. Jiang, C.D. Katchis, S. Kang, B.C. Dong, S. Li, and F.-Q. Zhou. 2018a. Lin28 Signaling Supports Mammalian PNS and CNS Axon Regeneration. *Cell Reports*. 24:2540-2552.e2546.

Wang, X.-W., Yang, S-G, Hu, M-W, Wang, R-Y, Zhang, C, Kosanam, A.R., Ochuba, A.J., Jiang, J-J, Luo, X, Qian, J, Liu, C-M, Zhou, F-Q. 2023. Histone methyltransferase EZH2 coordinates mammalian axon regeneration via epigenetic regulation of key regenerative pathways. *bioRxiv*. doi: https://doi.org/10.1101/2022.04.19.488817 （Journal of Clinical Investigation with minor revision).

Wang, X.W., S.G. Yang, C. Zhang, M.W. Hu, J. Qian, J.J. Ma, Y. Zhang, B.B. Yang, Y.L. Weng, G.L. Ming, A.R. Kosanam, Saijilafu, and F.Q. Zhou. 2020. Knocking Out Non-muscle Myosin II in Retinal Ganglion Cells Promotes Long-Distance Optic Nerve Regeneration. *Cell Rep*. 31:107537.

Wang, Y., L. Lin, H. Lai, L.F. Parada, and L. Lei. 2013. Transcription factor Sox11 is essential for both embryonic and adult neurogenesis. *Dev Dyn*. 242:638-653.

Wang, Z., V. Mehra, M.T. Simpson, B. Maunze, L. Holan, E. Eastwood, M.G. Blackmore, and I. Venkatesh. 2018b. KLF6 and STAT3 co-occupy regulatory DNA and functionally synergize to promote axon growth in CNS neurons. Cold Spring Harbor Laboratory.

Wang, Z., A. Reynolds, A. Kirry, C. Nienhaus, and M.G. Blackmore. 2015. Overexpression of Sox11 Promotes Corticospinal Tract Regeneration after Spinal Injury While Interfering with Functional Recovery. *The Journal of Neuroscience*. 35:3139-3145.

Weng, Y.-L., R. An, J. Cassin, J. Joseph, R. Mi, C. Wang, C. Zhong, S.-G. Jin, G.P. Pfeifer, A. Bellacosa, X. Dong, A. Hoke, Z. He, H. Song, and G.-L. Ming. 2017. An Intrinsic Epigenetic Barrier for Functional Axon Regeneration. *Neuron*. 94:337-346.e336.

Williams, P.R., L.I. Benowitz, J.L. Goldberg, and Z. He. 2020. Axon Regeneration in the Mammalian Optic Nerve. *Annual Review of Vision Science*. 6:195-213.

Wohl, S.G., and T.A. Reh. 2016. miR-124-9-9* potentiates Ascl1-induced reprogramming of cultured Müller glia. *Glia*. 64:743-762.

Yang, N., S. Chanda, S. Marro, Y.-H. Ng, J.A. Janas, D. Haag, C.E. Ang, Y. Tang, Q. Flores, M. Mall, O. Wapinski, M. Li, H. Ahlenius, J.L. Rubenstein, H.Y. Chang, A.A. Buylla, T.C. Südhof, and M. Wernig. 2017. Generation of pure GABAergic neurons by transcription factor programming. *Nature Methods*. 14:621-628.

Yang, S.G., C. Li, X. Peng, Z. Teng, C.M. Liu, and F.Q. Zhou. 2020. Strategies to promote long distance optic nerve regeneration. *Frontiers in Cellular Neuroscience*. in press.

Yang, S.G., X.W. Wang, C. Qian, and F.Q. Zhou. 2022. Reprogramming neurons for regeneration: The fountain of youth. *Prog Neurobiol*. 214:102284.

Yiu, G., and Z. He. 2006. Glial inhibition of CNS axon regeneration. *Nature Reviews Neuroscience*. 7:617-627.

Zaret, K.S., and J.S. Carroll. 2011. Pioneer transcription factors: establishing competence for gene expression. *Genes & Development*. 25:2227-2241.

Zhou, F.-Q., M.A. Walzer, and W.D. Snider. 2004. Turning On the Machine. *Neuron*. 43:1-2.

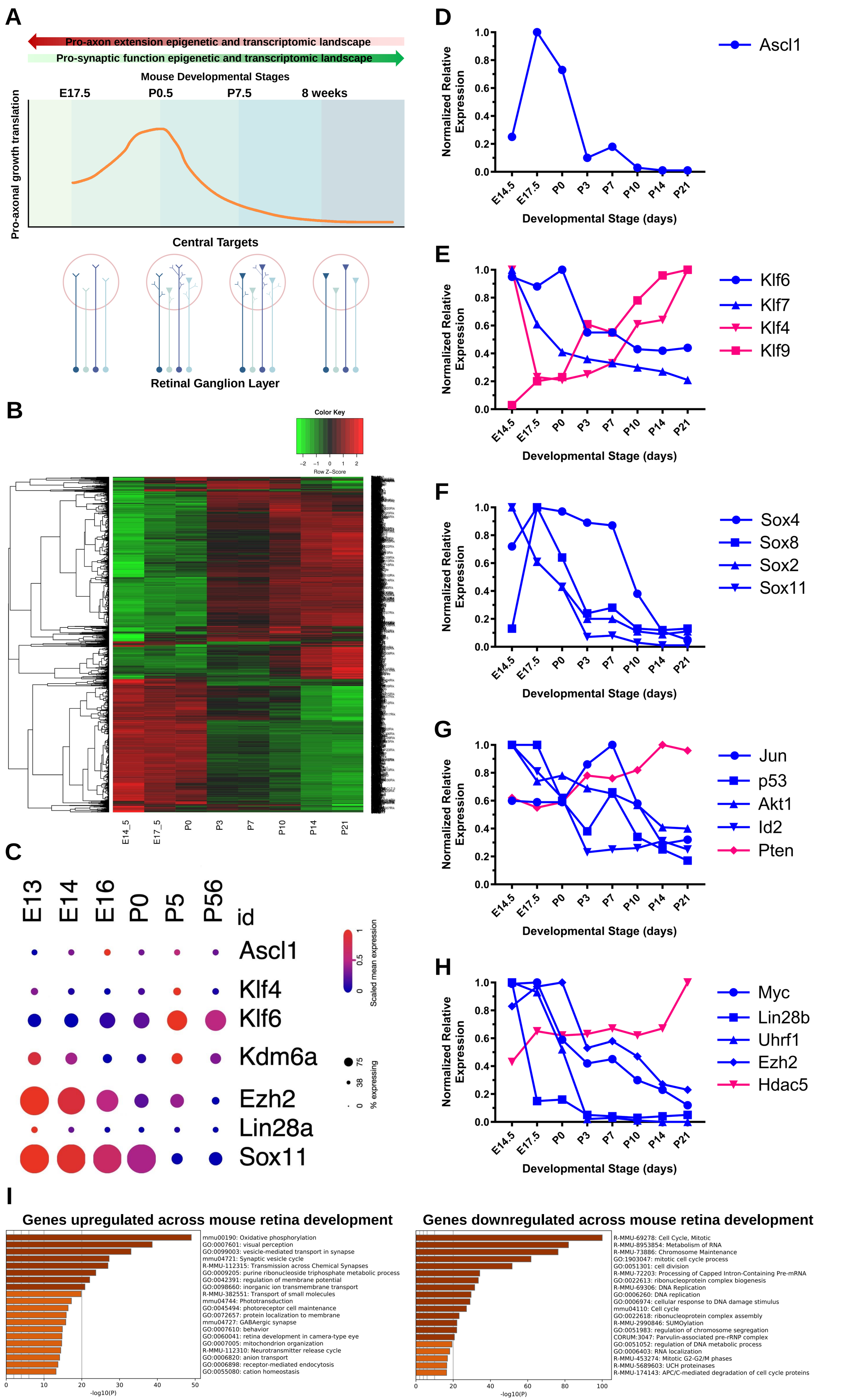
A
Pro-axon extension epigenetic and transcriptomic landscape
Pro-synaptic function epigenetic and transcriptomic landscape
Mouse Developmental Stages
E17.5
P0.5
P7.5
8 weeks
Pro-axonal growth translation
Central Targets
Retinal Ganglion Layer
B
Color Key
Row Z-Score
E14_5
E17_5
P0
P3
P7
P10
P14
P21
C
E14_5
E17_5
P0
P3
P7
P10
id
Ascl1
Klf4
Klf6
Kdm6a
Ezh2
Lin28a
Sox11
Scaled mean expression
% expressing
D
Ascl1
Normalized Relative Expression
Developmental Stage (days)
E
Klf6
Klf7
Klf4
Klf9
F
Sox4
Sox8
Sox2
Sox11
G
Jun
p53
Akt1
Id2
Pten
H
Myc
Lin28b
Uhrf1
Ezh2
Hdac5
I
Genes upregulated across mouse retina development
mmu00190: Oxidative phosphorylation
GO:0007601: visual perception
GO:0099003: vesicle-mediated transport in synapse
mmu04721: Synaptic vesicle cycle
R-MMU-112315: Transmission across Chemical Synapses
GO:0009205: purine ribonucleoside triphosphate metabolic process
GO:0042391: regulation of membrane potential
GO:0098660: inorganic ion transmembrane transport
R-MMU-382551: Transport of small molecules
mmu04744: Phototransduction
GO:0045494: photoreceptor cell maintenance
GO:0072657: protein localization to membrane
mmu04727: GABAergic synapse
GO:0007610: behavior
GO:0060041: retina development in camera-type eye
GO:0007005: mitochondrion organization
R-MMU-112310: Neurotransmitter release cycle
GO:0006820: anion transport
GO:0006898: receptor-mediated endocytosis
GO:0055080: cation homeostasis
-log10(P)
Genes downregulated across mouse retina development
R-MMU-69278: Cell Cycle, Mitotic
R-MMU-8953854: Metabolism of RNA
R-MMU-73886: Chromosome Maintenance
GO:1903047: mitotic cell cycle process
GO:0051301: cell division
R-MMU-72203: Processing of Capped Intron-Containing Pre-mRNA
GO:0022613: ribonucleoprotein complex biogenesis
R-MMU-69306: DNA Replication
GO:0006260: DNA replication
GO:0006974: cellular response to DNA damage stimulus
mmu04110: Cell cycle
GO:0022618: ribonucleoprotein complex assembly
R-MMU-2990846: SUMOylation
GO:0051983: regulation of chromosome segregation
CORUM:3047: Parvulin-associated pre-rRNP complex
GO:0051052: regulation of DNA metabolic process
GO:0006403: RNA localization
R-MMU-453274: Mitotic G2-G2/M phases
R-MMU-5689603: UCH proteinases
R-MMU-174143: APC/C-mediated degradation of cell cycle proteins
-log10(P)

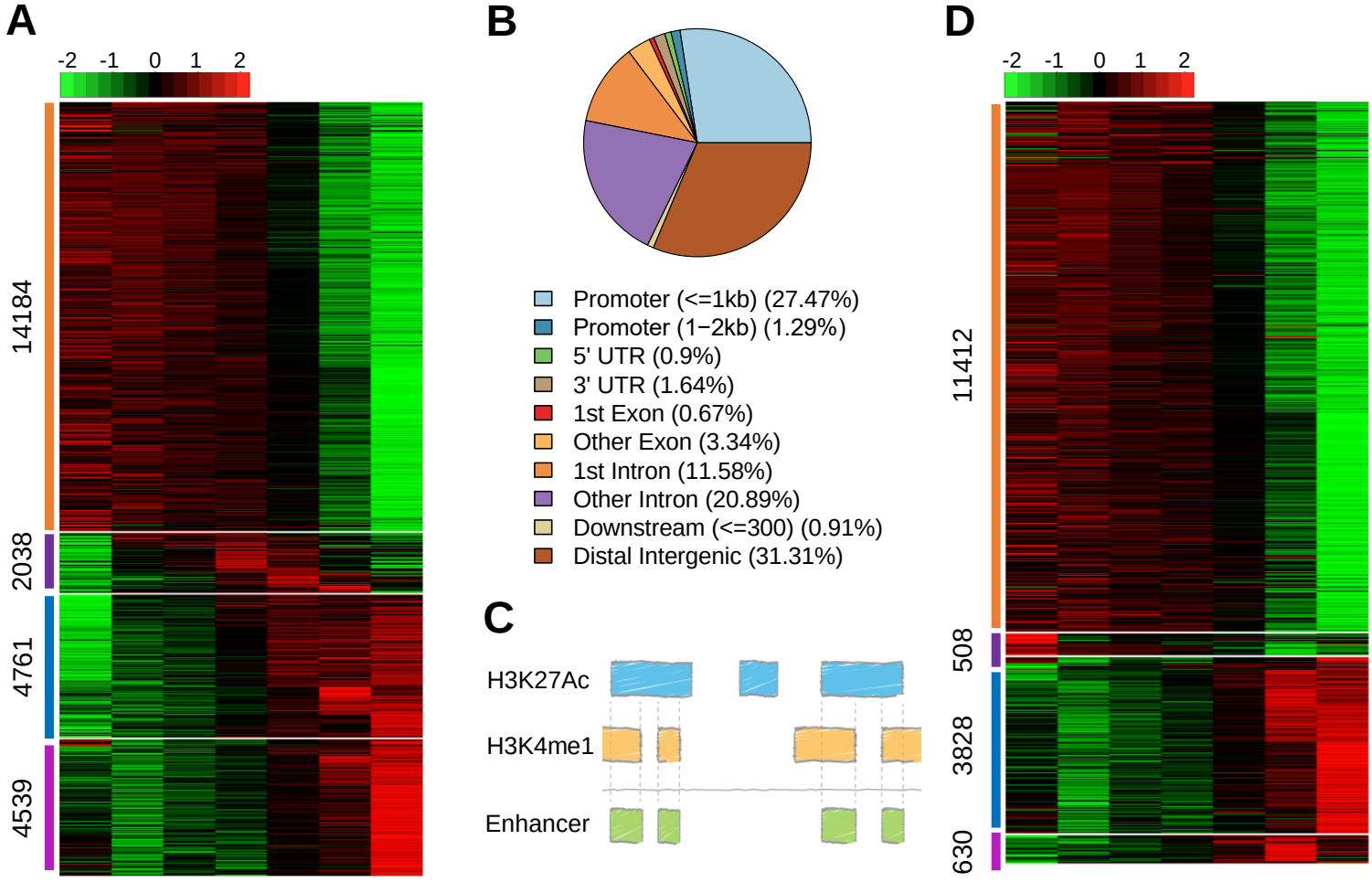
A
-2 -1 0 1 2
14184
2038
4761
4539
B
Promoter (<=1kb) (27.47%)
Promoter (1−2kb) (1.29%)
5' UTR (0.9%)
3' UTR (1.64%)
1st Exon (0.67%)
Other Exon (3.34%)
1st Intron (11.58%)
Other Intron (20.89%)
Downstream (<=300) (0.91%)
Distal Intergenic (31.31%)
C
H3K27Ac
H3K4me1
Enhancer
D
-2 -1 0 1 2
11412
508
3828
630

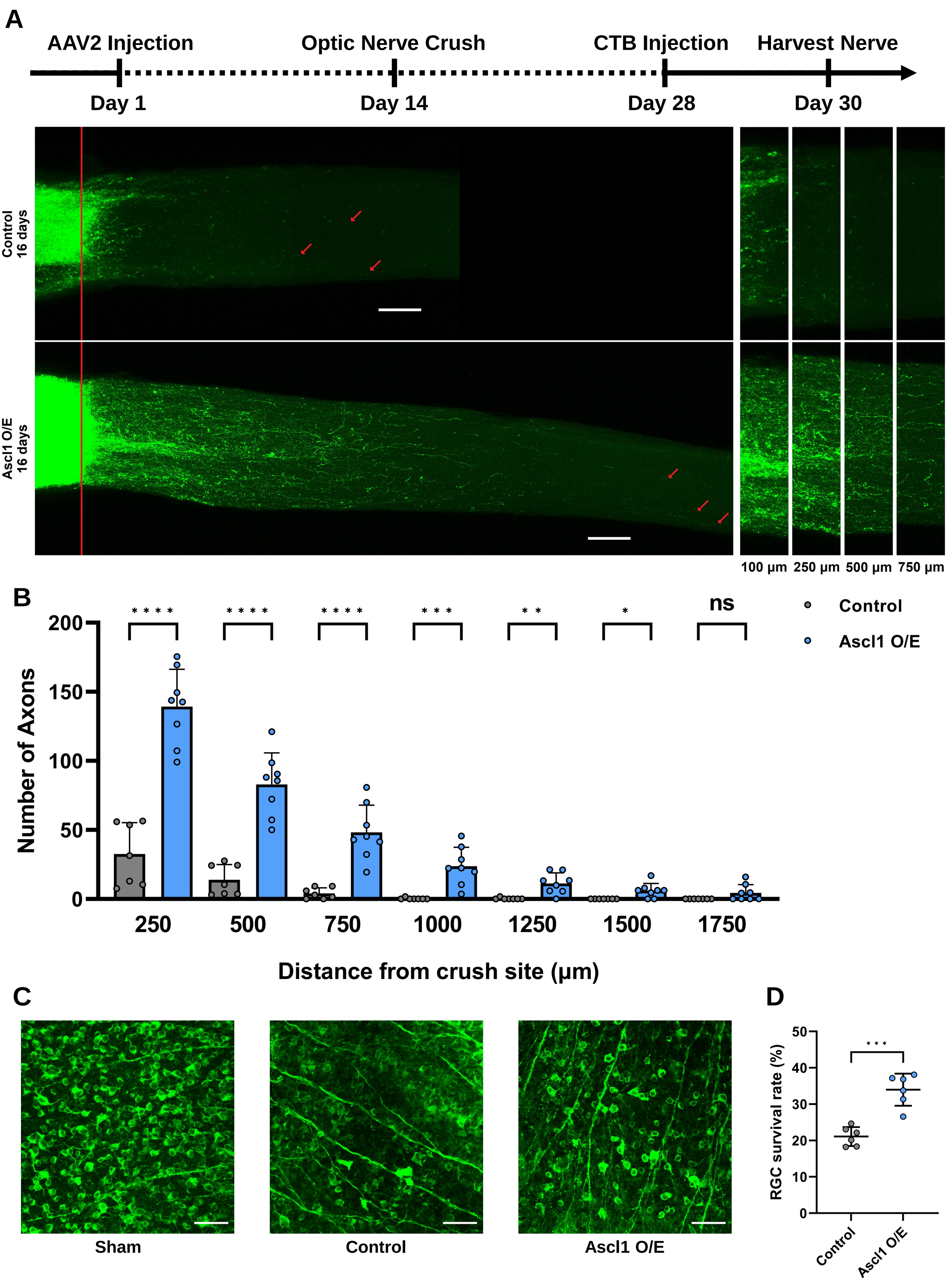
A
AAV2 Injection
Optic Nerve Crush
CTB Injection
Harvest Nerve
Day 1
Day 14
Day 28
Day 30
Control 16 days
Ascl1 O/E 16 days
100 µm
250 µm
500 µm
750 µm
B
ns
Control
Ascl1 O/E
Number of Axons
200
150
100
50
0
250
500
750
1000
1250
1500
1750
Distance from crush site (µm)
C
Sham
Control
Ascl1 O/E
D
RGC survival rate (%)
50
40
30
20
10
0
Control
Ascl1 O/E

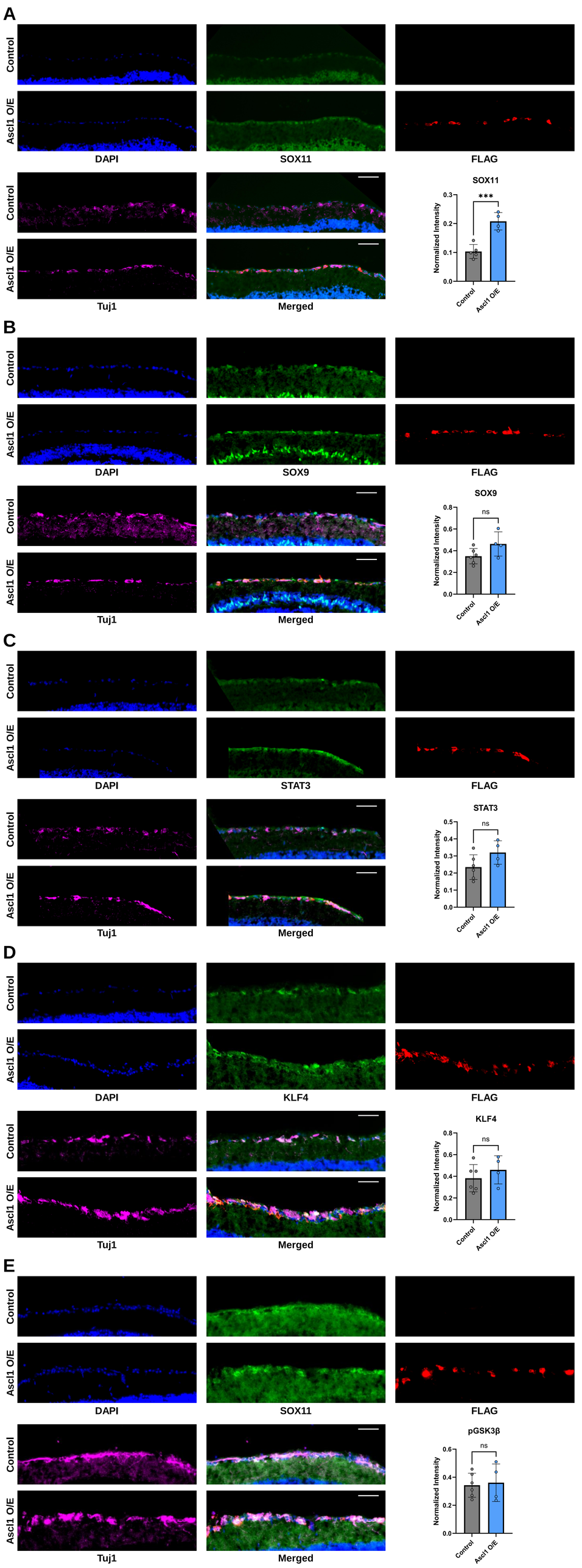
A
Control
Ascl1 O/E
DAPI
SOX11
FLAG
Control
Ascl1 O/E
Tuj1
Merged
SOX11
***
Normalized Intensity
0.3
0.2
0.1
0.0
Control
Ascl1 O/E
B
Control
Ascl1 O/E
DAPI
SOX9
FLAG
Control
Ascl1 O/E
Tuj1
Merged
SOX9
ns
Normalized Intensity
0.8
0.6
0.4
0.2
0.0
Control
Ascl1 O/E
C
Control
Ascl1 O/E
DAPI
STAT3
FLAG
Control
Ascl1 O/E
Tuj1
Merged
STAT3
ns
Normalized Intensity
0.5
0.4
0.3
0.2
0.1
0.0
Control
Ascl1 O/E
D
Control
Ascl1 O/E
DAPI
KLF4
FLAG
Control
Ascl1 O/E
Tuj1
Merged
KLF4
ns
Normalized Intensity
0.8
0.6
0.4
0.2
0.0
Control
Ascl1 O/E
E
Control
Ascl1 O/E
DAPI
SOX11
FLAG
Control
Ascl1 O/E
Tuj1
Merged
pGSK3β
ns
Normalized Intensity
0.6
0.4
0.2
0.0
Control
Ascl1 O/E

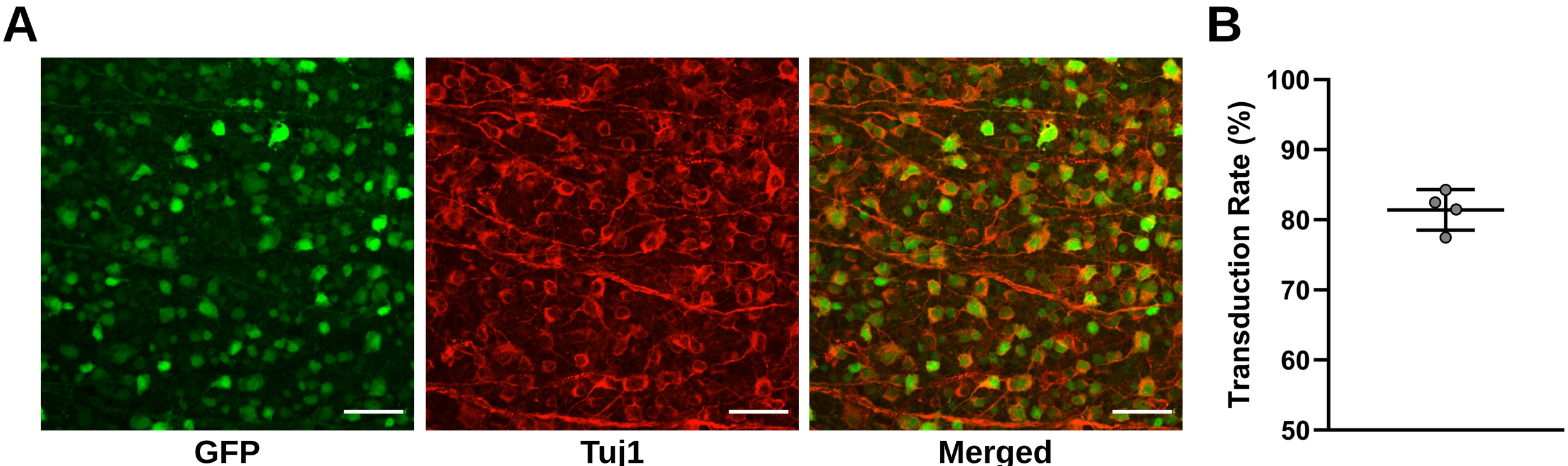
A
GFP
Tuj1
Merged
B
Transduction Rate (%)
100
90
80
70
60
50